Two Stage Optimization for Aerocapture Guidance

Zucchelli, E.M.; Hanasusanto, Grani A.; Brandon-Jones, A.; Mooij, E.

Important note
To cite this publication, please use the final published version (if applicable).
Please check the document version above.

Two-Stage Optimization for Aerocapture Guidance

Enrico M. Zucchelli[*], Grani A. Hanasusanto[†], and Brandon A. Jones[‡]
The University of Texas at Austin, Austin, TX, 78705

Erwin Mooij[§]
Delft University of Technology, Delft, The Netherlands, 2629 HS

This paper proposes a two-stage optimization approach for aerocapture guidance. In classical entry guidance systems, deterministic optimization is used. Large-scale and short-scale density perturbations may strongly affect the performance of the guidance system, and variations in those are usually not accounted for when computing the command. In this work, perturbations that affect the trajectory at future time-steps are taken into consideration when computing the commanded bank angle. The chosen command is optimal based on a set of possible future perturbations, after the observation of which, a correction can be made. Both two-stage stochastic and two-stage robust optimization are proposed as a solution. In a Monte Carlo analysis consisting of 50 runs, the two-stage robust optimization guidance outperforms an optimal, deterministic, numeric predictor-corrector guidance. Excluding one outlier, also the two-stage stochastic optimization makes the guidance perform better than an optimal deterministic numeric predictor-corrector. With either approach, the computational demands are increased by about thirty times compared to an optimal numeric predictor-corrector. Much of the computation time increase may be reduced by parallelization. On the other hand, the extensive tuning required for the optimal numeric predictor-corrector is not needed for the two-stage optimization guidance, making this approach conceptually more robust. Better modeling of the environment may help further improve the performance. Finally, an approximation to the two-stage robust optimization approach is developed. The guidance has computational requirements only four times larger than those of the optimal numeric predictor-corrector guidance, but can be parallelized into two threads, and, except for two outliers, it offers improved performance.

Nomenclature

a	semi-major axis, m
C_D	drag coefficient
C_L	lift coefficient
D	drag, N
e	eccentricity
g_δ	latitudinal component of the gravity, m/s^2
g_r	radial component of the gravity, m/s^2
i	inclination, rad
L	lift, N
m	mass, kg
$\dot{q}$	heat-flux at stagnation point, W/s^2
Q	integrated heat-load, J/s^2
r	radial distance, m
R_e	equatorial radius of the primary, m
R_N	nose radius, m
t	time, s
V	relative speed, m/s

---

[*]Graduate Student, Aerospace Engineering and Engineering Mechanics, 2617 Wichita St.

[†]Assistant Professor, Operations Research and Industrial Engineering, 204 E Dean Keeton Street.

[‡]Assistant Professor, Aerospace Engineering and Engineering Mechanics, 2617 Wichita St.

[§]Associate Professor, Aerospace Engineering, Kluyverweg 1.

1

β	inverse of scale-height, 1/m
γ	relative flight-path angle, rad
δ	latitude, rad
μ	gravitational parameter of the primary, m^3/s^2
ρ	atmospheric density, kg/m^3
σ	bank angle, rad
τ	longitude, rad
χ	heading, rad
ω_{cb}	rotational rate of the primary body, rad/s

Subscripts

0	initial conditions
a	apoapsis
f	final
p	periapsis
opt	optimal

Superscripts

| $\star$ | target |

I. Introduction

Aerocapture is an atmospheric maneuver that may consistently reduce the use of propelled thrust upon arrival to a different planet [1]. To properly achieve orbital capture, a spacecraft has to reduce its specific energy relative to the destination planet. Traditional orbital capture involves the use of rockets to slow down the spacecraft and make the orbit elliptic; with aerocapture, the latter result is achieved by plunging into the atmosphere of the planet in a controlled manner and exiting again. Rockets are required to raise the periapsis of the orbit, as well as to correct the apoapsis altitude, but the amount of ΔV needed is usually one order of magnitude lower or even less than what is needed for normal capture. Because of Tsiolkovsky's rocket equation, which shows that the initial mass (and thus cost) of a rocket is exponential in the ΔV of the entire mission, aerocapture may enable several missions otherwise impossible with current rocket technology [2], and make many other mission scenarios considerably more efficient. The benefits of aerocapture can be, depending on the mission design [3]: 1) decreased initial mass, and thus reduced cost of the mission; 2) shorter travel time, since, for equal mass, a higher V_∞ is possible at capture; 3) increased payload mass.

The goal of an aerocapture is to reduce the energy of the spacecraft approaching the destination planet on a hyperbolic orbit, and to obtain a final stable orbit around the primary. One usually wants an orbit with a prespecified altitude and eccentricity. A specific orbit inclination is also usually targeted, but for simplicity this is neglected in this work; this is without loss of generality, since the lateral motion affects the maneuver in a usually negligible way, and is often controlled by a separate logic.

A scheme of the aerocapture maneuver is depicted in Fig. 1. During an aerocapture the spacecraft plunges into the atmosphere; once a critical dynamic pressure is reached, bank angle modulation begins. This consists of opportunely directioning the bank angle σ, and thus the direction of the lift force. The bank angle is modulated such that the total ΔV required to obtain the desired final orbit is minimized. The modulation of the bank angle ensures that the spacecraft exits the atmosphere, and that the path constraints are satisfied. Path constraints include limits on peak deceleration and peak heat-flux, as well as total heat-load. Heat-flux and heat-load include radiative and convective heat transfer. After the spacecraft exits the atmosphere, it coasts until apoapsis is reached; a propelled periapsis raise maneuver of magnitude ΔV_1 is performed, and, half an orbit later, a final correction of magnitude ΔV_2 is performed again. The latter correction is required in case the first maneuver of ΔV_1 occurs at an altitude that is neither the desired final periapsis or apoapsis.

The bank angle is the angle between the local vertical plane and the direction of the lift vehicle, and can be changed by rotating the vehicle around the velocity direction. It has been proven that, for a wide range of aerocapture maneuvers, apoapsis targeting implies ΔV minimization [4] if a constant bank angle throughout the trajectory is the only decision variable. By application of optimal control theory it has been shown [5–7] that, for some reasonable simplifying assumptions, all the path constraints are minimized by the same trajectory that, at the same time, achieves the required apoapsis altitude and minimizes $\Delta V_{tot} = \Delta V_1 + \Delta V_2$. Such trajectory is obtained by bang-bang control: the lift has to
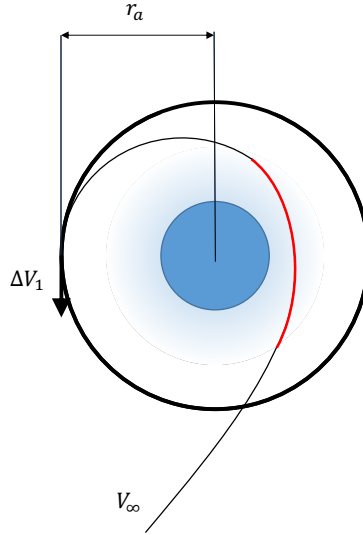
Fig. 1   Scheme of an aerocapture. In red is the atmospheric part of the maneuver.

be directed fully upwards, and, after a switching time t_s, fully downwards. Because of this, the optimal trajectory is very unstable: if any perturbation occurs after the switching time t_s, there is no margin for correction, as the control is already saturated. The fact that the path constraints are minimized by the same trajectory minimizing the ΔV implies that the guidance logic can be designed to minimize just ΔV_{tot}; if the constraints are still not satisfied, it is because the constraints could not have been satisfied to begin with.

Several algorithms exist for aerocapture guidance. Analytic Predictor-Correctors (APCs) [8–10] are a family of guidance algorithms that are a direct heritage of the Apollo skip guidance [11]. For most of these methods, the algorithm computes a constant direction of the bank angle σ needed to reach a target periapsis. The bank angle is sought via analytic approximations of the trajectory. The computed bank angle is then the one commanded until the next guidance call. Updates (usually with a frequency of 1 Hz) are needed because of errors caused by uncertainties unaccounted for, and errors caused by mismodeling of the dynamics. The majority of the mismodeling error in APCs comes from the fact that analytic solutions usually neglect the Coriolis acceleration, second-order terms, and involve the use of a very simple exponential model for the atmospheric density. While being extremely fast, APCs are also rather inaccurate, since an aerocapture maneuver is much less stable than a skip entry, and analytic approximations are coarse. Moreover, because of the inherent instability of the optimal trajectory, they are even less practical if an optimal solution is sought. Numeric Predictor-Correctors (NPCs) [4, 12] operate similarly to APCs, but the trajectory is computed numerically. Because of this, modelling errors are highly reduced; however, errors caused by uncertainties in the model remain. In the majority of NPCs, only a constant bank angle is sought, reducing the problem to a single variable root solver: hence, the only difference between an APC and most NPCs is the method by which the trajectory is propagated. Thanks to the fact that it is known that an optimal aerocapture is very closely obtained with a bang-bang control, an attempt to achieve optimal guidance has been made with the Fully Numerical Predictor-Corrector Aerocapture Guidance (FNPAG) [5]. In that work an NPC-like guidance is divided into two phases. During the first phase, the commanded bank angle is lift-up, with $\sigma = 0$ or very close to zero, and a switching time t_s is computed: the switch is between a lift-up phase and a lift-down phase. The switch time is recomputed with a frequency of 1 Hz; if the computed switch time is negative, or is predicted to occur within one second from the current time-step, a shift to the second phase occurs. In that phase, an algorithm similar to the normal NPC operates. Because of the above mentioned instability of the trajectory, combined with the large uncertainties of the model, the bank angle σ used in phase 1 to propagate the portion of flight after t_s is not full lift-down, but a margin is applied. This margin is empirically tuned and a function of initial conditions only, V_0 and γ_0. The tuning of this parameters requires several iterations of Monte Carlo analysis for each entry conditions [5].

The goal of this paper is to propose an optimal aerocapture guidance that takes future uncertainty into account. This provides a robust guidance, while at the same time offering optimality, without any tuning required. Section II describes the aerocapture problem. Section III briefly describes the two-stage stochastic programming framework, and Sec. IV

3

describes the approach proposed for this work. Section V displays the results obtained via simulation, and Sec. VI concludes the paper.

II. Aerocapture Dynamics

A spacecraft in motion in the atmosphere of an ellipsoidal celestial body evolves as follows, in spherical coordinates, in a planet fixed reference frame [13]:

$$\dot{V} = -\frac{D}{m} - g_r \sin \gamma - g_\delta \cos \gamma \cos \chi + \omega_{cb}^2 r \cos \delta (\sin \gamma \cos \delta - \cos \gamma \sin \delta \cos \chi), \tag{1}$$

$$V\dot{\gamma} = \frac{L \cos \sigma}{m} - g_r \cos \gamma + g_\delta \sin \gamma \cos \chi + 2\omega_{cb}V \cos \delta \sin \chi + \frac{V^2}{r} \cos \gamma + \\ + \omega_{cb}^2 r \cos \delta (\cos \gamma \cos \delta - \sin \gamma \sin \delta \cos \chi), \tag{2}$$

$$V \cos \gamma \dot{\chi} = \frac{L \sin \sigma}{m} + g_\delta \sin \chi + 2\omega_{cb}V(\cos \gamma \sin \delta - \sin \gamma \cos \delta \cos \chi) + \\ + \frac{V^2}{r} \cos^2 \gamma \tan \delta \sin \chi + \omega_{cb}^2 r \cos \delta \sin \delta \sin \chi, \tag{3}$$

$$\dot{r} = V \sin \gamma, \tag{4}$$

$$\dot{\tau} = \frac{V \sin \chi \cos \gamma}{r \cos \delta}, \tag{5}$$

$$\dot{\delta} = \frac{V \cos \gamma \cos \chi}{r}, \tag{6}$$

where V is the velocity of the spacecraft, γ is the flight-path angle, χ is the heading angle of the spacecraft, δ is the latitude of the spacecraft, r is the distance of the spacecraft from the center of the body, and τ is the latitude. σ is the spacecraft bank angle, which is the only control input to the system, ω_{cb} is the rotation rate of the celestial body, m is the mass of the spacecraft, $D = 1/2\rho V^2 S C_D$ and $L = 1/2\rho V^2 S C_L$ are drag and lift forces respectively, C_L and C_D are the coefficients of drag and lift respectively, and ρ is the air density. g_r and g_δ are the two components of the gravity field if the oblateness of the primary is accounted for:

$$g_\delta = \frac{3}{2} \frac{\mu}{r^2} \left(\frac{R_e}{r}\right)^2 \sin 2\delta,$$

$$g_r = \frac{\mu}{r^2} \left(1 - \frac{3}{2} J_2 \left(\frac{R_e}{r}\right)^2 \left(3 \sin^2 \delta - 1\right)\right), \tag{7}$$

where R_e is the equatorial radius of the planet. This model is simplified as it does not include any gravitational perturbations other than the one caused by the J_2 coefficient of the planet, nor any perturbations caused by the wind. Nonetheless, Eqs. (1)-(6), combined with the appropriate atmospheric and aerodynamic models, are sufficient to predict the motion of a spacecraft in an atmosphere with satisfying results for the purpose of a guidance logic, and are thus the equations generally used in NPCs.

By coordinate transformations, one can link the above model to Keplerian elements. If the target orbit is circular with semi-major axis $a^\star$, and the exit orbit has semi-major axis a and eccentricity e, such that the apoapsis radius of the exit orbit is $r_a = a(1 + e)$, then the ΔV needed to raise the periapsis is

$$\Delta V_1 = \sqrt{2\mu} \left\| \sqrt{\frac{1}{r_a} - \frac{1}{r_a + a^\star}} - \sqrt{\frac{1}{r_a} - \frac{1}{2a}} \right\|, \tag{8}$$

and the ΔV to correct the apoapsis altitude is

$$\Delta V_2 = \sqrt{2\mu} \left\| \sqrt{\frac{1}{2a^\star}} - \sqrt{\frac{1}{a^\star} - \frac{1}{r_a + a^\star}} \right\|. \tag{9}$$

4

The sum of the two post-atmospheric burns $\Delta V_{tot} = \Delta V_1 + \Delta V_2$ is the cost function that an optimal aerocapture guidance aims to minimize.

The major source of uncertainty in this problem are the air density ρ and the lift-to-drag ratio between the coefficients of lift C_L and of drag C_D. The aerodynamic coefficients are function of the Mach number (which is a function of velocity and local speed of sound, which in turn is a function of air temperature and air composition), and are rather difficult to estimate even if all variables are known; in NPCs, C_L and C_D are usually modeled as constants. In simplified models used for aerocapture guidance, the density is just a function of altitude; on Earth, the US76 Standard Atmospheric Model [14] is often used for NPCs. In reality however, density is also a function of latitude, longitude, and time, as well as of solar flux. Moreover, atmosphere density prediction comes with very large uncertainty, even on Earth when the most sophisticated models are used, and thus the true density is going to differ from the mean estimate. To partly account for modeling errors in density and lift-to-drag ratio NPCs often use first-order fading memory filters for the density [5]:

$$\tilde{\rho}_L^{(n+1)} = \tilde{\rho}_L^{(n)} + (1-\beta)\left(\rho_L - \tilde{\rho}_L^{(n)}\right), \qquad 0 \le \beta \le 1, \tag{10}$$

$$\tilde{\rho}_D^{(n+1)} = \tilde{\rho}_D^{(n)} + (1-\beta)\left(\rho_D - \tilde{\rho}_D^{(n)}\right), \qquad 0 \le \beta \le 1, \tag{11}$$

with

$$\rho_L = L/L_m, \qquad \rho_D = D/D_m,$$

where L and D are the sensed lift and drag forces respectively, and L_m and D_m are the lift and drag according to the models. $\tilde{\rho}_L$ and $\tilde{\rho}_D$ then multiply the lift and the drag respectively during the entirety of the propagated trajectory. These filters only estimate the currently sensed atmospheric density, and assume that future deviations from the density will keep constant. In reality, large changes in variations from the models can be expected at future time-steps because of the presence of atmospheric perturbations, which are modeled as random even in the most accurate atmospheric models. Because the system is nonlinear, future uncertainty in any of the above mentioned parameters causes an asymmetry in outcomes, and thus reasoning in terms of expected value of those parameters leads to a biased decision. For this reason, stochastic optimization is proposed.

III. Two-Stage Optimization

Optimization under uncertainty is the branch of optimization that concerns the minimization of a specified metric of a quantity of interest, or cost, Z, which is a function of not only of the decision variables, but also of a random variable, or uncertain parameter, $\xi \in \Xi$, unknown at the time of the optimization. In stochastic optimization such metrics are usually either the expected value of the quantity of interest, or a weighted sum of the expected value and of the standard deviation of said quantity of interest. Conversely, in robust optimization the metric to be optimized is the worst-case cost: it is assumed that the unknown parameter ξ is adversarial instead of random. That requires optimizing assuming that the worst-case scenario will occur, and results in a min-max problem.

Two-stage optimization, either stochastic or robust, concerns problems where decisions can be made at two different epochs in time. First, a decision is made; then, the realization of the random variable is revealed, and a second decision can be made. The second decision is the solution to a deterministic optimization problem; the problem depends on the first decision variable and on the realization of the random variable. Hence, two-stage stochastic optimization solves the following problem [15]:

$$z = \inf_{\mathbf{x} \in \mathcal{X}} f(\mathbf{x}) + \mathbb{E}[Z(\mathbf{x}, \boldsymbol{\xi})] \tag{12}$$
$$\text{s.t.} \quad \mathbf{g}(\mathbf{x}) = \mathbf{0}$$
$$\mathbf{h}(\mathbf{x}) \le \mathbf{0}$$

where $\mathcal{X} \subseteq \mathbb{R}^n$, $\boldsymbol{\xi} \in \Xi \subseteq \mathbb{R}$ is the random variable, $\mathbf{g} : \mathbb{R}^n \to \mathbb{R}^m$ and $\mathbf{h} : \mathbb{R}^n \to \mathbb{R}^l$. In addition:

$$Z(\mathbf{x}, \boldsymbol{\xi}) = \inf_{\mathbf{y} \in \mathcal{Y}} f_2(\mathbf{x}, \boldsymbol{\xi}, \mathbf{y}) \tag{13}$$
$$\text{s.t.} \quad \mathbf{g}_2(\mathbf{x}, \boldsymbol{\xi}, \mathbf{y}) = \mathbf{0}$$
$$\mathbf{h}_2(\mathbf{x}, \boldsymbol{\xi}, \mathbf{y}) \le \mathbf{0}$$

5

with $\mathcal{Y} \subseteq \mathbb{R}^{n_2}$, $\mathbf{g}_2 : \mathbb{R}^n \times \mathbb{R} \times \mathbb{R}^{n_2} \to \mathbb{R}^{m_2}$ and $\mathbf{h}_2 : \mathbb{R}^n \times \mathbb{R} \times \mathbb{R}^{n_2} \to \mathbb{R}^{l_2}$. $Z(\mathbf{x}, \boldsymbol{\xi})$ is the recourse function. If $Z(\mathbf{x}, \boldsymbol{\xi})$ is feasible for every possible choice of $\mathbf{x}$ and $\boldsymbol{\xi}$, than the problem is said to have full recourse. Two-stage robust optimization is similar, but Eq. (12) is substituted with

$$z = \inf_{\mathbf{x} \in \mathcal{X}} f(\mathbf{x}) + \sup_{\boldsymbol{\xi} \in \Xi} Z(\mathbf{x}, \boldsymbol{\xi}) \tag{14}$$
$$\text{s.t.} \quad \mathbf{g}(\mathbf{x}) = \mathbf{0}$$
$$\mathbf{h}(\mathbf{x}) \leq \mathbf{0}$$

The two-stage optimization problem is generally NP-hard for continuous random variables and for linear problems, and usually requires approximation methods to be solved. Examples of approximations are Monte Carlo sampling and linear (or quadratic) decision rules. In Monte Carlo sampling, the expected value of the cost, or the worst case cost, is approximated as a sum of S scenarios, and the problem ends up being a larger optimization problem, with $n + n_2 \times S$ decision variables. With linear decision rule methods, the second decision variable y is simplified as a linear function of the random variable $\boldsymbol{\xi}$ with q parameters ($q = 2$ for linear, $q \geq 2$ for piece-wise linear approximations), and thus the problem becomes a single-stage problem with $n + q$ decision variables. Besides a few exceptions, this solution requires some kind of sampling too. For linear problems, Benders decomposition is an alternative method that can solve the problem, but is rarely used in nonlinear problems; for continuous random variables, it does require sampling as well [16].

IV. Two-Stage Optimization Guidance

A. Background

Three guidance logics are presented in this section. The first two, described in Sec. IV.B, are called 2SGuid and 2RGuid and solve a two-stage stochastic and a two-stage robust problem respectively. The third, presented in Sec. IV.D and called 2RDGuid, solves a two-stage robust optimization problem with additional simiplifying assumptions.

To have a guidance that is optimal under uncertainty, single-stage stochastic programming would not be suitable to the problem. This is because the bank angle is extremely sensitive to perturbations: a bank angle history that is optimal for some conditions, would in most cases lead to a skipout or a crash for different conditions. Hence, finding a bank angle trajectory that leads to feasible solutions for all conditions is not possible. For this reason, two-stage optimization is proposed; in two-stage optimization, a different bank angle history can be selected for different realizations of the perturbations, as long as a few initial time-steps are shared among all scenarios. The two-stage optimization guidance aims at computing those initial time-steps such that the solution is optimal, either in a robust or in a stochastic sense. As previously mentioned, the major source of uncertainty in aerocapture is caused by atmospheric perturbations. The uncertainty in density is difficult to model exactly, as it may vary according to both small-scale and large-scale perturbations. Moreover, the variation in density from a nominal value is not constant in time and space, and is in reality a stochastic process, characterized by an infinite number of random variables. To simplify, the density perturbation is modeled as a function of a single random variable throughout the trajectory. Otherwise, too many samples would be needed. Hence, since with this approach we only have a single random variable, a grid sampling approach is used instead of Monte Carlo approach. An additional problem comes from the fact that the deviation of density from nominal is not revealed for the whole trajectory all at once, but instead it is revealed while the trajectory moves forward. Hence, the correct solution would require a multi-stage stochastic program, which is the solution to the stochastic optimal control problem, and is intractable even for the simplest application. When solving for a two-stage problem, the problem is simplified such that all stages after the second are condensed into the same stage. To simplify further, it is assumed that the perturbation deviation happening along the whole trajectory is revealed as soon the first decision is made.

At every guidance call, the first decision variable is the constant bank angle to be commanded until the guidance is called again, whereas the second decision variable is the constant bank angle to be commanded for the remainder of the trajectory. Because of the structure of the guidance problem, the second decision variable is never actually implemented, and is only needed to compute the first-stage variable. Because the command is continuously updated while the random variables are revealed, one ends up solving an approximation to a multi-stage stochastic program by iteratively solving a two-stage program.

B. Two-stage Stochastic and Two-stage Robust Guidance

Two guidance logics are proposed, one making use of two-stage stochastic optimization, 2SGuid, and the second one, 2RGuid, making use of two-stage robust optimization. The only random variable (or uncertain parameter) considered in the optimization is the density, since it is the variable whose uncertainty causes the largest differences in outcome during the trajectory. The variables whose initial conditions are uncertain, such as γ_0 or V_0, are not considered either, because they are not unknown anymore once the guidance is called. Another large source of uncertainty is the evolution of the lift-to-drag ratio L/D, which may change in unforeseeable ways during the trajectory; this is a stochastic process too. The possible variation of L/D during the trajectory is relatively small and has overall a smaller impact on the final outcome than the variation expected in the density has; it is thus neglected at the current stage of development. The following two-stage stochastic program is solved at each call of 2SGuid:

$$z = \inf_{\sigma_1} \mathbb{E}[\Delta V_{tot}^{\star}(\sigma_1, \delta\rho)] \tag{15}$$

where $\delta\rho \in \Xi = [-37.5\%, 0\%, +50\%]$ is a random variable, and all outcomes are assumed to have equal probability. The values are picked such to cover a large interval of perturbations. The difference in density multiplies the whole density profile by a factor that differs from the one currently being observed. The effective density multiplier used by the guidance system is a function of time too:

$$\rho_m = 1 + \delta\rho(1 - e^{-t/T}), \tag{16}$$

where T is a time constant. In addition:

$$\Delta V_{tot}^{\star}(\sigma_1, \delta\rho) = \inf_{\sigma_2 \in [0, \pi]} \Delta V_{tot}(\sigma_1, \sigma_2, \delta\rho) \tag{17}$$

$$s.t. \quad \mathbf{x}_{i2} = \mathbf{x}_{f1}(\sigma_1), \tag{18}$$

where $\mathbf{x}_{i2}$ is the vector of initial conditions of the spacecraft for stage 2, and $\mathbf{x}_{f1}$ is the vector of final conditions at the end of stage 1. Recalling Eq. (12), here we have $f(\mathbf{x}) = 0, \forall x$. The so formulated problem does not always have full recourse: depending on the trajectory, it is possible that some choices of σ_1 may lead to infeasible solutions for some instances of $\delta\rho$ in the second stage. The non-feasibility is accounted for with large penalties on the cost function. This way, full recourse is ensured.

For the 2RGuid, that solves the robust two-stage optimization, everything is the same except for Eq. (15), which is substituted with:

$$z = \inf_{\sigma_1} \sup_{\delta\rho \in \Xi} \Delta V_{tot}^{\star}(\sigma_1, \delta\rho) \tag{19}$$

Because of the strong nonlinearities and discontinuities of the problem, both guidance logics solve the recourse function by bisection, since, as stated in Sec. II, the inner optimization can be reduced to a root-solving problem. Bisection is needed to ensure robustness since the problem is highly nonlinear. The outer problem is instead solved by the golden section method, also in this case because of the strong nonlinearity of the problem. The command σ_1 is only sought between in the intersection between the intervals $[0, \pi]$ and $[\sigma_0 - \Delta\sigma, \sigma_0 + \delta\sigma]$, where σ_0 is the bank angle state at the time of computation, and $\delta\sigma$ is the change in bank angle that can be covered at each guidance call. To be conservative, $\delta\sigma$ is set equal to $30°$. The golden section method requires that only one optimum is in the interval in which the variable is sought. This has not been proven to be true; however, given that 1) the interval is limited compared to the full domain, and 2) that the first-stage variable has a much smaller impact on the performance than the second variable has, it is reasonable that only a single optimum exists, and that is indeed what has been empirically found for all tested cases.

Figure 2 depicts the schematics of the two-stage optimization guidance. For each scenario s, a different value of $\sigma_2^{(s)}$ is selected, but all scenarios share a common value for σ_1. In the two-stage stochastic guidance, σ_1 and $\sigma_2^{(s)}, s = 1 : S$ are chosen such that the weighed average of all outcomes is minimized. In the two-stage robust guidance, σ_1 and $\sigma_2^{(s)}, s = 1 : S$ are chosen such that the worst-case of all outcomes is minimized. The trajectories are propagated according to the same models described in Sec. II. σ_1 is commanded for only a short period of time. Notably, the rotational motion between σ_0 (the current bank angle), σ_1, and $\sigma_2^{(2)}$ is not modeled as instantaneous. This is because, as shown in Ref. [6], the rotational motion has non-negligible duration compared to the whole aerocapture, and failure to account for that motion may lead to very large errors.
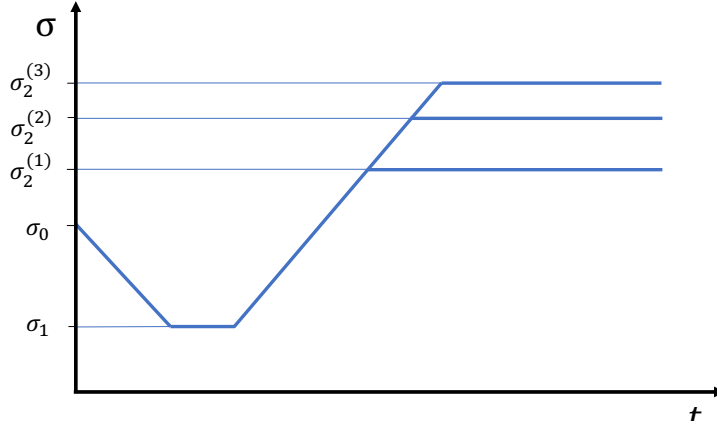
Fig. 2   Scheme of the two-stage optimization guidance logic.

To compute σ_1 with an accuracy higher than $0.5°$, a value comparable to the deadband of the spacecraft, about ten iterations of the outer loop are needed. This is because the domain of possible angles is limited to $\pm 30°$ of the bank angle at the time where the guidance is called: any value farther away would not be reachable within the time-frame anyway. The inner loop requires instead about 20 iterations, and needs to be computed three times per outer loop iteration. That is because the search domain is $[0°, 180°]$, and also because higher accuracy in the bank angle is needed: while the guidance will not actually execute the command σ_2 computed in the recourse function, a small error in σ_2 may lead to a large error in ΔV, and thus the choice of the first stage variable may be affected by numeric errors in the second stage if σ_2 is not computed with very high accuracy. Because of this, the total number of trajectory propagations is around 720 per guidance call, compared to a normal NPC usually requiring about 15 trajectories. Hence, the full two-stage guidance requires about 40 times the computational effort of a normal NPC. As it will be shown in Sec. IV.D, the number can be reduced by exploiting the structure of the problem.

C. Optimality

Consider for now the above described guidance logics, but neglecting the perturbations and the uncertainties: this is a guidance that solves a deterministic two-variable optimization problem, where the variables are σ_1 and σ_2. The goal of this section is to show that, in a deterministic sense, such guidance is optimal. The two-stage optimization process then accounts for perturbations on top of that. As stated in Sec. II, the optimal aerocapture guidance follows a bang-bang, full lift-up, full lift-down trajectory. Such a trajectory is not allowed by this guidance method, and thus it may seem that the logic cannot allow an optimal trajectory. In fact, the switching time is fixed, and the optimizer can only compute the values of the bank angle before and after the switching time. Nonetheless, because of the structure of the problem, the following relation is true:

$$\text{sign}\left(\frac{\partial \sigma_2}{\partial \sigma_1}\right) = -1. \tag{20}$$

This is trivially justified: since a specified final altitude is targeted in the second stage, if the bank angle σ_1 causes the spacecraft to deplete more energy during the first stage, then less energy has to be depleted in the second stage. Eq. (20) implies that, if the final conditions can be achieved by two different sequences of σ_1 and σ_2, then the sequence that has the smallest value of σ_1 also has the largest value of σ_2. Said sequence then provides a ΔV_{tot} lower than the other one, since bang-bang control trajectories are optimal, and is then preferred to the latter one from the guidance logic. Hence, depending on the spacecraft state, either $\sigma_1 = 0$ or $\sigma_2 = \pi$. Because σ_1 is only implemented for a very short period of time in the guidance logic, $\sigma_2 = \pi$ only when, if an actual bang-bang control were applied, the switching time t_s is really close in time. Consequently, $\sigma_1 = 0$ until t_s is reached, as in an optimal bang-bang trajectory, even if the guidance does not explicitly plan a bang-bang trajectory.

Table 1 Computational requirements of the proposed guidance logics (and NPC for reference).

Guidance	$\approx$ n. of iterations	Max n. of parallel threads
NPC	15	1
2SGuid	720	3
2RGuid	720	3
2SGuid (faster)	360	3
2RGuid (faster)	360	3
2RDGuid (3 scenarios)	180	3
2RDGuid (2 scenarios)	80	2

D. Computational Efficiency

The golden section optimization method searches for an optimum by seeking the minimum in an increasingly smaller interval. Because of Eq. (20), for each scenario, while the interval for σ_1 decreases, the interval for σ_2 can be decreased too. This ends up in a reduction of, overall, a factor of 2 in the number of total trajectory computations. This is what is done for the two-stage stochastic guidance 2SGuid and two-stage robust guidance 2RGuid, which then result in the propagation of about 360 trajectories, taking approximately 20 times the computational requirements of the normal NPC.

An alternative approach, called 2RDGuid is possible thanks to the considerations about optimality from the previous section. Since an optimal trajectory, when no perturbations are considered, has either $\sigma_1 = 0$ or $\sigma_2 = \pi$, only trajectories of this kind are sought, for all the various scenarios. Hence, the problem reduces to s different optimization problems (s being the number of different scenarios), all with one single variable: the variable is either σ_1 if $\sigma_2 = \pi$, or σ_2 if $\sigma_1 = 0$. This greatly simplifies the problem, but provides a non-unique value of σ_1. At this point, for all the optimal σ_1 so far computed, an optimal σ_2 is computed for all scenarios. Finally, the commanded value σ_1 is the command that provides the minimum worst-case scenario ΔV. Hence, in the 2RDGuid a two-stage robust optimization problem is solved, where the first stage variable is discretized. The set of first stage variable considered includes only the values that are optimal for each scenario when they are considered singularly. The 2RDGuid provides a worse solution than the 2RGuid by construction, since it solves the same problem as the 2RGuid but only chooses the solution from a limited set of commands. On the other hand, this approach reduces the computational requirements to a total of 9 times the computational requirements of a normal NPC, since only three scenarios are evaluated for 3 different values of σ_1. An additional simplification is the reduction of the total number of scenarios to just 2, the two most extreme ones: the worst case scenario is most likely to happen for an extreme perturbation, and Ξ is reduced to $[-37.5\%, +50\%]$. In this case, the cost reduces to being approximately only 4 times that of an NPC. Table 1 compares the computational time of the guidance logics proposed in this paper.

Alternative methods that may be used to improve numerical tractability include the possibility of using analytic predictors instead of numeric ones, or a multi-fidelity approach [17, 18], by which in this case analytic solutions may be combined with numeric solutions for high accuracy, high speed solutions.

V. Results

The three guidance systems are tested on 50 simulated aerocapture scenarios for an Apollo-like vehicle approaching the outer atmosphere layers at 120 km of altitude, with an inertial velocity of approximately 12 km/s. The initial flight-path angle γ_0 is random and uniformly distributed between -6.5° and -5°. The atmospheric density is also random, and includes both long-scale and short-scale perturbations; the mean follows the profile of the Earth GRAM 2010 [19] model. The true aerodynamic coefficients are interpolated as a function of Mach number using Apollo data [20]. Figure 3 shows the ΔV and the apoapsis altitude as a function of the entry angle achieved with the two-stage stochastic optimization guidance. As a comparison, Fig. 4 shows the ΔV obtained for the same scenarios, but with the OAK guidance from Ref. [6], which is a modification of the optimal FNPAG that requires less tuning. Except for one outlier, the stochastic guidance outperforms on average the optimal aerocapture guidance. The OAK guidance requires an average ΔV of 120.2 m/s, whereas the two-stage stochastic guidance requires an average ΔV of 123.4 m/s; however, neglecting the outlier, the average ΔV decreases to 117.4 m/s. This is noteworthy, since the stochastic optimization method does not require any tuning, but only a coarse knowledge of the uncertainty in the atmospheric model. The

outlier is most likely caused by modeling issues, which need to be solved in future work. Another noteworthy detail is the apoapsis altitude obtained with the two methods: the stochastic guidance is, even neglecting the outlier, much less accurate in apoapsis targeting. Nonetheless, in terms of ΔV_{tot}, the guidance still outperforms optimal deterministic approaches for many cases where it is less accurate in terms of apoapsis altitude. This is because of a combination of two factors: 1) the perturbations are taken into account in the guidance logic and 2) a bang-bang trajectory is always allowed with this scheme: whereas the FNPAG or the OAK only compute a constant bank angle after $t \geq t_s$, the two-stage stochastic guidance still allows for different values of σ_1 and σ_2, and is thus better performing, since it will always command a smaller bank angle, as long as it is safe to do so.
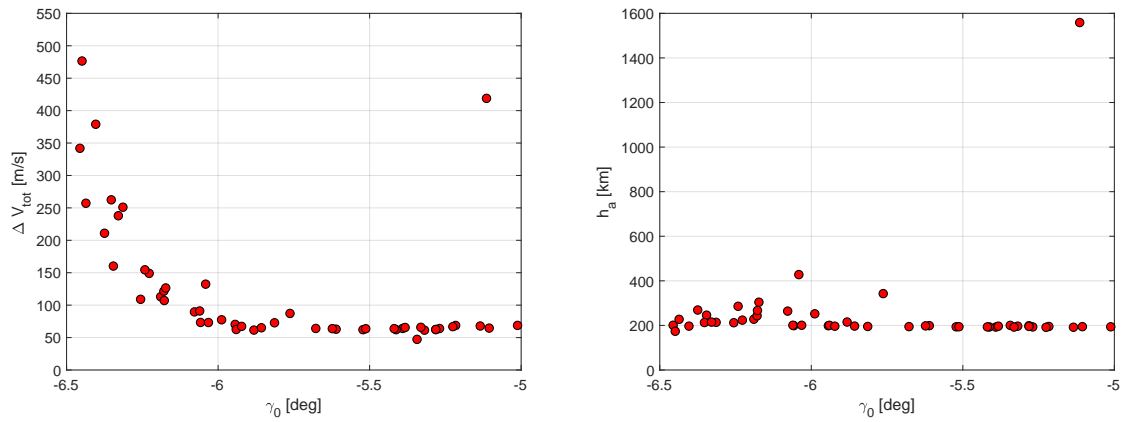

Fig. 3 ΔV_{tot} **(left) and apoapsis altitude (right) obtained as a function of initial flight-path angle γ_0 for the 2-stage stochastic optimization guidance.**
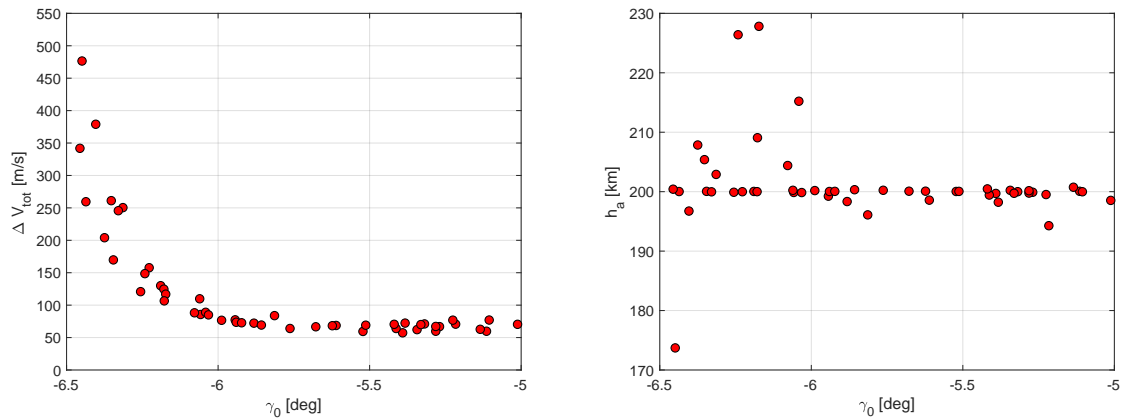

Fig. 4 ΔV_{tot} **(left) and apoapsis altitude (right) obtained as a function of initial flight-path angle γ_0 for the OAK guidance.**

Figure 5 shows the performance of the two-stage robust optimization approach. This approach is more robust than the two-stage stochastic optimization guidance, but still has a few occurrences where it is outperformed by an NPC, for the largest of which the difference is about 40 m/s. Overall, the 2RGuid outperforms the NPC by 4 m/s. Reduction in frequency and magnitude of the outliers is expected with this approach since two-stage robust optimization aims at mitigating the worst-case scenarios. Figure 6 shows the bank angle histories of the 50 scenarios for the two-stage robust optimization guidance on the left and for the OAK guidance on the right. It is easy to notice how the OAK guidance ends up saturating with a bank angle at 0 degrees at the end, much more often than the two-stage robust guidance: this is indication of the fact that the bang-bang control is not exploited as much. In constrast, the two-stage robust guidance always saturates at σ =180 degrees, which is optimal as long as the apoapsis altitude is not too far from the target one.
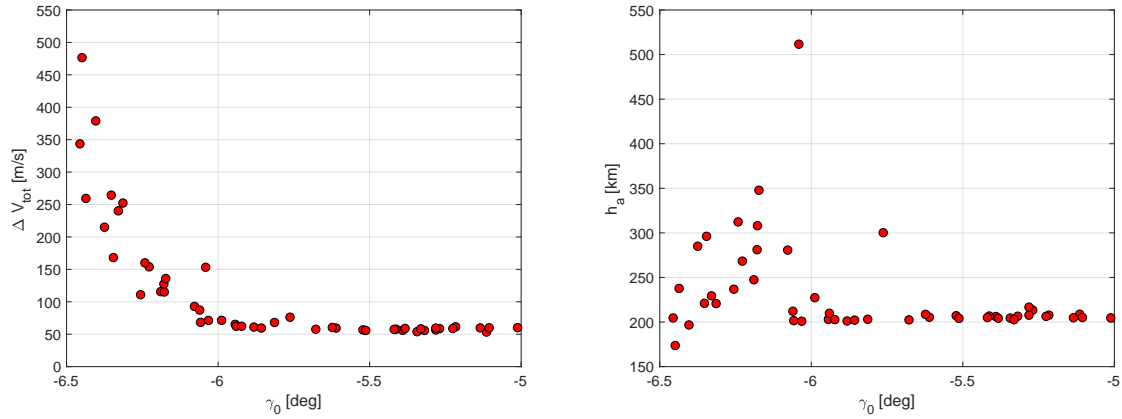
Fig. 5 ΔV_{tot} **(left) and apoapsis altitude (right) obtained as a function of initial flight-path angle** γ_0 **for the 2-stage robust optimization guidance (2RGuid).**
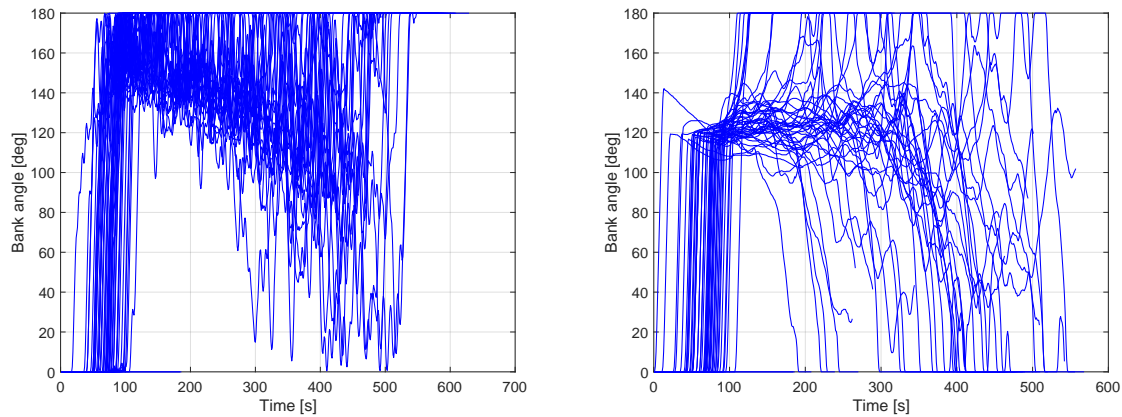

Fig. 6 **Bank angle histories for the two-stage robust optimization guidance (left) and for the OAK guidance (right).**

Fig. 7 shows the performance of the 2RDGuid guidance that approximates the two-stage optimization guidance by discretization. The performance is comparable to that of the two-stage optimization guidance, but it is obtained with a computational cost that is only four times as large as that of the OAK guidance, and can be parallelized in up to two threads. Including the outliers, this guidance is outperformed by the OAK guidance by 5 m/s, excluding the outlier, this guidance outperforms the OAK guidance by 1.5 m/s. Crucially, these results are obtained without any tuning, and are theoretically more robust, since their results are rooted in the theory of stochastic optimization. Nonetheless, a more accurate modeling of the perturbations is needed. Finally, Table 2 summarizes the results.

VI. Conclusions

The two-stage stochastic and two-stage robust opimization guidance for aerocapture were developed and tested. The two-stage robust optimization guidance outperforms current state-of-the-art optimal, deterministic NPC, the FNPAG. With the exclusion of one outlier, also the two-stage stochastic approach outperforms the FNPAG. Such results are obtained without any tuning required, and are conceptually more robust than any deterministic optimization-based guidance. The robust optimization approach is better performing than the stochastic optimization approach, and is less subject to outliers, as expected. Both methods have computational requirements that are approximately 20 to 30 times larger than those of the FNPAG, but the computation can be parallelized up to three times. An approximation to the robust optimization method is also proposed. Such approximation only requires four times as much the computational accuracy
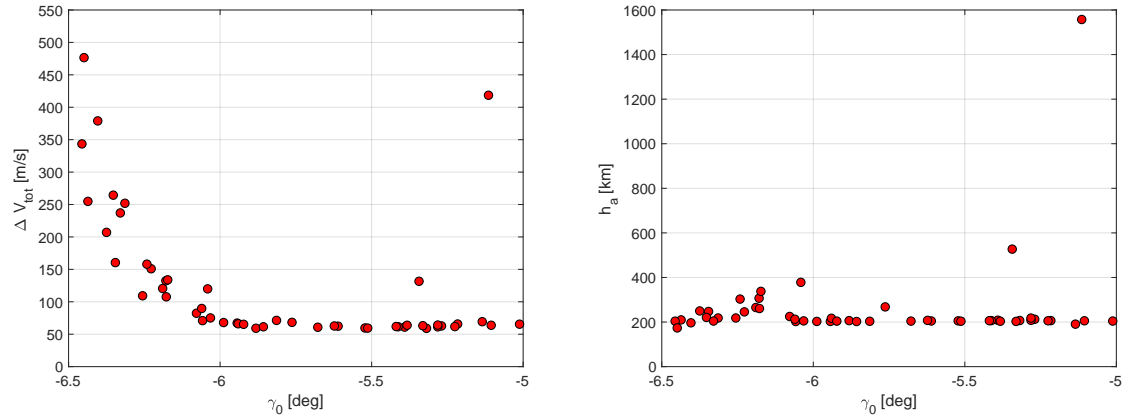
Fig. 7 ΔV_{tot} **(left) and apoapsis altitude (right) obtained as a function of initial flight-path angle** γ_0 **for the discretized robust optimization guidance (2RDGuid) with two scenarios only.**

Table 2 Summary of the results for the proposed guidance logics (and NPC for benchmark).

Guidance	$\approx$ n. of iterations	Tuning	Mean ΔV [m/s]	Mean ΔV, w/o outlier [m/s]
NPC	15	Yes	119.0	119.9
2SGuid (faster)	360	No	123.4	117.1
2RGuid (faster)	360	No	114.7	115.6
2RDGuid (3 scenarios)	180	No	122.5	116.2
2RDGuid (2 scenarios)	80	No	123.8	117.5

of the FNPAG, and can be parallelized into up to two threads, and performs similarly to the two-stage optimization approach

The results can be improved through better modeling of the environment. The vector of variations $\delta\rho$ should be state dependent: if the spacecraft is already encountering extreme variations of the density, it is more likely that the density would reverse towards the mean in the future time-steps, and thus the values of $\delta\rho$, and their corresponding probability, should change accordingly. Variations in not only the density but also in the lift-to-drag ratio may be included in the second-stage. Finally, methods to make the two-stage stochastic and two-stage robust guidance faster may be investigated. Possible candidates are pure analytic solutions (it was recently showed that near-optimality can be achieved even with analytic predictor-correctors [21]), or by a combination of analytic and numeric propagators through multi-fidelity approaches such as in Refs. [17, 18].

References

[1] Cruz, M., "The aerocapture vehicle mission design concept," *Conference on Advanced Technology for Future Space Systems*, A79-34701, Hampton, VA, 1979.

[2] Hall, J. L., Noca, M. A., and Bailey, R. W., "Cost-benefit analysis of the aerocapture mission set," *Journal of Spacecraft and Rockets*, Vol. 42, No. 2, 2005, pp. 309–320.

[3] Spilker, T. R., Adler, M., Arora, N., Beauchamp, P. M., Cutts, J. A., Munk, M. M., Powell, R. W., Braun, R. D., and Wercinski, P. F., "Qualitative Assessment of Aerocapture and Applications to Future Missions," *Journal of Spacecraft and Rockets*, Vol. 56, No. 2, 2019, pp. 536–545.

[4] Lafleur, J. M., "The conditional equivalence of δv minimization and apoapsis targeting in numerical predictor-corrector Aerocapture guidance," *NASA Johnson Space Center, Houston*, 2011.

12

[5] Lu, P., Cerimele, C. J., Tigges, M. A., and Matz, D. A., "Optimal aerocapture guidance," *Journal of Guidance, Control, and Dynamics*, Vol. 38, No. 4, 2015, pp. 553–565.

[6] Zucchelli, E., and Mooij, E., "Minimum radiative heat-load aerocapture guidance with attitude-kinematics constraints," *AIAA Guidance, Navigation, and Control Conference*, AIAA 18-1319, Kissimmee, FL, 2018.

[7] Sigal, E., and Guelman, M., "Optimal aerocapture with minimum total heat load," *Proceedings of the 52nd International Astronautical Congress*, 2001.

[8] Cerimele, C., and Gamble, J., "A simplified guidance algorithm for lifting aeroassist orbital transfer vehicles," *23rd Aerospace sciences meeting*, AIAA 1985-348, Reno, NV, 1985.

[9] Masciarelli, J., Rousseau, S., Fraysse, H., and Perot, E., "An analytic aerocapture guidance algorithm for the Mars Sample Return Orbiter," *Atmospheric flight mechanics conference*, AIAA 2006-6394, Keystone, CO, 2000.

[10] Hamel, J.-F., and De Lafontaine, J., "Improvement to the analytical predictor-corrector guidance algorithm applied to Mars aerocapture," *Journal of guidance, control, and dynamics*, Vol. 29, No. 4, 2006, pp. 1019–1022.

[11] Moseley, P., "The Apollo entry guidance: a review of the mathematical development and its operational characteristics," *Task MSC/TRW A-220*, 1969.

[12] Powell, R. W., and Braun, R. D., "Six-degree-of-freedom guidance and control analysis of Mars aerocapture," *Journal of Guidance, Control, and Dynamics*, Vol. 16, No. 6, 1993, pp. 1038–1044.

[13] Mooij, E., *The motion of a vehicle in a planetary atmosphere*, Delft University Press, 1997.

[14] Atmosphere, U. S., *US standard atmosphere*, National Oceanic and Atmospheric Administration, 1976.

[15] Shapiro, A., Dentcheva, D., and Ruszczyński, A., *Lectures on stochastic programming: modeling and theory*, SIAM, 2014.

[16] Infanger, G., "Monte Carlo (importance) sampling within a Benders decomposition algorithm for stochastic linear programs," *Annals of Operations Research*, Vol. 39, No. 1, 1992, pp. 69–95.

[17] Narayan, A., Gittelson, C., and Xiu, D., "A Stochastic Collocation Algorithm with Multifidelity Models," *SIAM Journal on Scientific Computing*, Vol. 36, No. 2, 2014, pp. A495–A521. https://doi.org/10.1137/130929461.

[18] Jones, B. A., and Weisman, R., "Multi-Fidelity Orbit Uncertainty Propagation," *Acta Astronautica*, Vol. 155, 2019, pp. 406–417. https://doi.org/10.1016/j.actaastro.2018.10.023.

[19] Justh, H., Justus, C., and Keller, V., "Global reference atmospheric models, including thermospheres, for mars, venus and earth," *AIAA/AAS Astrodynamics Specialist Conference and Exhibit*, AIAA 2006-6394, 2006.

[20] Moss, J., Glass, C., and Greene, F., "DSMC simulations of Apollo capsule aerodynamics for hypersonic rarefied conditions," *9th AIAA/ASME Joint Thermophysics and Heat Transfer Conference*, AIAA 2006-3577, San Frnacisco, CA, 2006.

[21] Cihan, I. H., and Kluever, C. A., "Analytical Earth-Aerocapture Guidance with Near-Optimal Performance," *Journal of Guidance, Control, and Dynamics*, 2020.